DR2013023

Low rates of bedrock outcrop erosion in the central Appalachian Mountains inferred from *in situ* ^{10}Be

Eric W. Portenga
Department of Geology
University of Vermont
Burlington, VT 05405

Paul R. Bierman
Department of Geology and Rubenstein School of the Environment and Natural Resources
University of Vermont
Burlington, VT 05405

Donna M. Rizzo
College of Engineering and Mathematical Sciences
University of Vermont
Burlington, VT 05405

Dylan H. Rood
Center for Accelerator Mass Spectrometry
Lawrence Livermore National Laboratory
Livermore, CA 94550

and

Earth Research Institute
University of California
Santa Barbara, CA 93106

now at

Scottish Universities Environmental Research Centre (SUERC)
East Kilbride G75 0QF, UK

Cosmogenic Nuclide Background

The development of accelerator mass spectrometry (Elmore and Phillips, 1987) allowed geomorphologists to estimate denudation rates directly by measuring small concentrations of cosmogenic isotopes, such as ^{10}Be, in a variety of earth materials (Bierman and Nichols, 2004; Gosse and Phillips, 2001). Cosmogenic nuclides were first widely used as erosion rate monitors in the 1980s (Cerling, 1990; Craig and Poreda, 1986; Kurz, 1986; Nishiizumi et al., 1991). ^{10}Be has been measured in over 400 samples (Portenga and Bierman, 2011) from bedrock outcrops, including numerous studies concerning passive-margin and arid-region landscape change (e.g. Bierman and Caffee, 2001; Bierman and Caffee, 2002; Cockburn et al., 2000); however, ^{10}Be measurements in fluvial sediments have seen far wider use, with over 1,100 measurements (Portenga and Bierman, 2011) published to date (e.g. Bierman et al., 2005; DiBiase et al., 2010; Safran et al., 2005; Schaller et al., 2001).

Methods

ArcGIS Sampling Strategy

We developed a field sampling strategy in ESRI ArcGIS (vers. 9.3) incorporating bedrock geology maps for Maryland, Pennsylvania, Virginia, and West Virginia, downloaded from the USGS Geological Map Database (http://ngmdb.usgs.gov/). We located outcrops of quartz-rich lithologies based upon lithologic descriptions provided by each map. State and National Park and Forest boundaries within the Potomac and Susquehanna River Basins were added to the map as they typically protect and preserve natural landforms and provide easy access to features, including bedrock outcrops, by means of hiking trails and access roads. We cross-referenced names of potential sampling sites within the park and forest boundaries with

gazetteers, road atlases, topographic maps, and internet photos to assess the suitability, quality, and accessibility of bedrock outcrops prior to field work. Knowing exactly where to go before entering the field area was paramount to a more efficient field season and the successful collection of over fifty usable outcrop samples, many from remote locations.

Laboratory Methods

Samples returned to the University of Vermont where they were crushed, ground, magnetically separated, and sieved; only the nonmagnetic 250–850 μm grain-size fraction was retained. Samples were then etched in a series of dilute HCl, HNO_3, and HF acids following the methods of Kohl and Nishiizumi (1992), and if necessary, mineral grains were separated according to density. Samples were tested for quartz-purity using inductively coupled plasma optical emission spectrometry (ICP-OES) before a final, 10-day etch in weak HNO_3 and HF.

About twenty grams of sample were weighed into digestion bottles and a known amount of SPEX 1000 ppm ^{9}Be carrier solution (~250 μg ^{9}Be) was added to each sample. Samples were run in batches of twelve that included one full process blank and eleven samples. The sample and carrier were then digested in concentrated HF. Samples were dried down four times in $HClO_4$, treated with HCl and redissolved in 6N HCl. Anion column chromatography removed Fe from each sample; subsequent cation column chromatography separated B, Ti, and Al from Be. A beryllium-hydroxide gel was precipitated with NH_4OH and the gels were dried, flame oxidized, and mixed with Nb in a 1:1 molar ratio before being packed into stainless steel cathodes. Specific quartz preparation methods can be found at the University of Vermont Cosmogenic Nuclide Laboratory website (http://www.uvm.edu/cosmolab/?Page=methods.html).

Isotopic Analysis and Data Reduction

$^{10}Be/^{9}Be$ ratios were measured by AMS at Lawrence Livermore National Laboratory in April, 2010. All samples were normalized to standard 07KNSTD3110, with a reported $^{10}Be/^{9}Be$ ratio of 2.85×10^{-11} (Nishiizumi et al., 2007). Measured sample ratios ranged from 3.9×10^{-14} to 3.8×10^{-12}, and AMS measurement precisions, including propagated blank corrections, ranged from 0.8 to 3.5%, averaging 1.5% (1σ, Table 1). Samples were prepared in seven separate batches using two different SPEX 1000 ppm carrier solutions. The process blanks for three batches with the first carrier are 1.88×10^{-14}, 1.90×10^{-14}, and 1.80×10^{-14}. For the second carrier, the blanks were 1.31×10^{-14}, 1.27×10^{-14}, 1.26×10^{-14}, and 1.25×10^{-14}. The representative carrier average blank $^{10}Be/^{9}Be$ ratio was subtracted from the measured ratio for each sample. Blank corrections averaged 4% of measured ratios.

Calculating Erosion Rates

^{10}Be concentrations were derived from measured ratios of $^{10}Be/^{9}Be$ and used to calculate erosion rates using the CRONUS on-line cosmogenic erosion rate calculator (Balco et al., 2008). The calculator (vers. 2.1) is updated with the most widely accepted values for constants (vers. 2.2.1) and also accounts for the muogenic production of ^{10}Be (vers. 1.1). Using the samples' geographic coordinates, elevation, thickness, density (2.7 g cm^{-3}), and ^{10}Be concentration, CRONUS calculates model erosion rates. We used erosion rates corrected for latitude and elevation based on the scaling schemes of Lal (1991) and Stone (2000). Results are normalized to a high-latitude and sea-level ^{10}Be production rate of 4.96±0.43 atoms g^{-1} yr^{-1} (Balco et al., 2008). Errors reported in our analyses are 1σ AMS measurement errors and are propagated through the CRONUS calculations.

Figure A1.

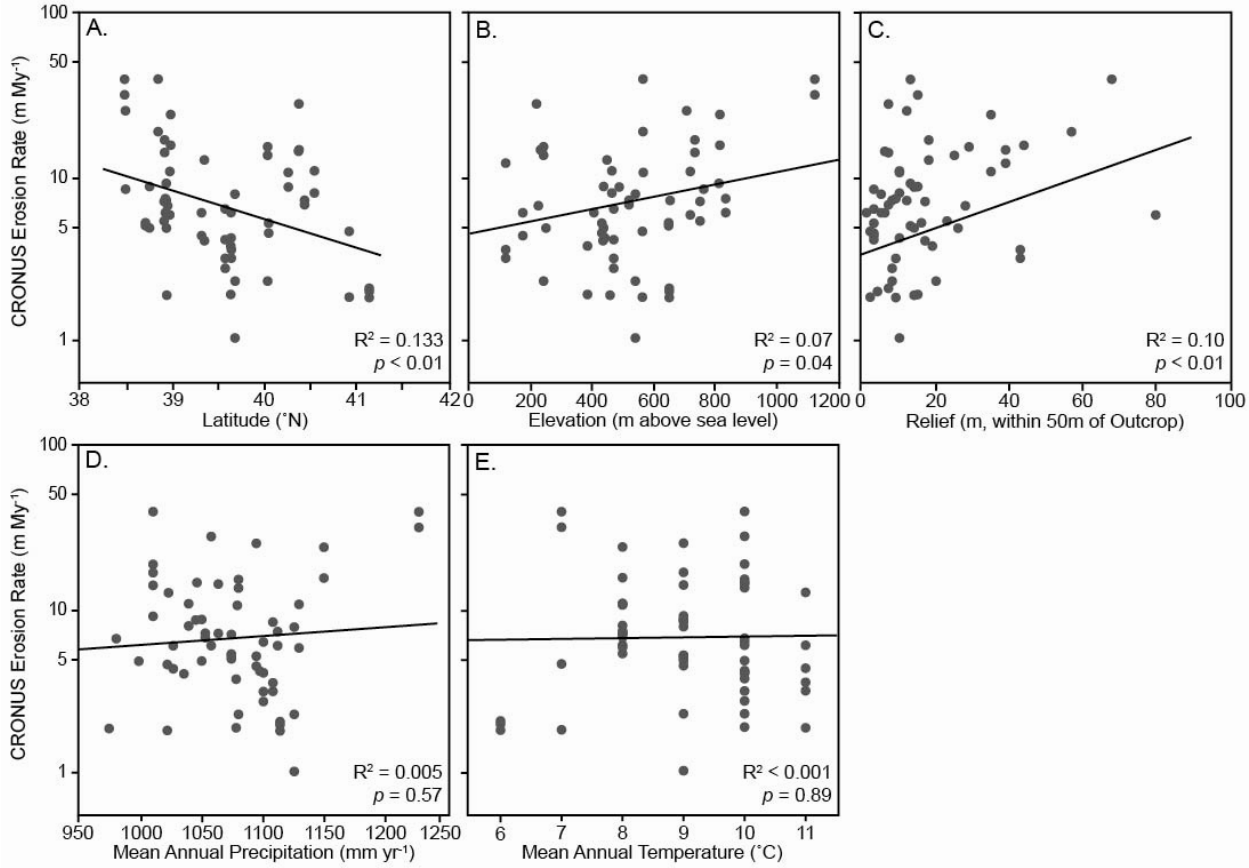

Figure A1. Bivariate correlations between bedrock outcrop erosion rate inferred from ^{10}Be as it relates to A: Latitude (°N), B: Elevation (m above sea level), C: Relief (m, within a 50m radius of each sampled outcrop), D: Mean Annual Precipitation (mm yr^{-1}, Hijmans et al., 2005), and E: Mean Annual Temperature (°C, Hijmans et al., 2005).

TABLE A1. SAMPLE PARAMETER DATA

Sample ID	LLNL Be ID*	Longitude (°W)	Latitude (°N)	Lithology	Thickness (cm)	Elevation (masl)†	Relief (m)†§	MAP (mm yr^{-1})#	MAT (°C)#	Climate Zone**	Physiographic Province
Main Ridgeline Outcrops											
EPP01	BE28738	77.73640	39.31041	Quartzite	3	349	3	1028	11	Dfa	Blue Ridge
EPP02	BE28739	77.73652	39.31003	Quartzite	2	350	6	1028	11	Dfa	Blue Ridge
EPP04	BE28740	77.45293	39.56918	Quartzite	5	415	9	1104	10	Dfa	Blue Ridge
EPP05	BE28741	77.45421	39.56810	Quartzite	5	433	3	1104	10	Dfa	Blue Ridge
EPP06	BE28742	77.45427	39.56794	Quartzite	7	434	3	1104	10	Dfa	Blue Ridge
EPP07	BE28743	77.45306	39.56895	Quartzite	6	418	8	1104	10	Dfa	Blue Ridge
EPP08	BE28744	77.43211	39.62942	Quartzite	2	407	19	1081	10	Dfa	Blue Ridge
EPP09	BE28745	77.43271	39.62911	Quartzite	2	419	15	1081	10	Dfa	Blue Ridge
EPP10	BE28746	77.43777	39.63340	Phyllite	5	419	10	1101	10	Dfa	Blue Ridge
EPP11	BE28747	77.43788	39.63204	Phyllite	3	394	5	1060	10	Dfa	Blue Ridge
EPP12	BE28749	77.71630	39.34103	Quartzite	3	438	18	1024	11	Dfa	Blue Ridge
EPP13	BE28750	77.71601	39.34185	Quartzite	2	429	17	1037	10	Dfa	Blue Ridge
EPP14	BE28751	77.52410	39.67564	Quartzite	4	524	10	1130	9	Dfa	Blue Ridge
EPP15	BE28752	77.52350	39.67712	Quartzite	4	544	8	1130	9	Dfa	Blue Ridge
EPP16	BE28753	77.52499	39.67506	Quartz Vein	4	527	5	1130	9	Dfa	Blue Ridge
EPP17	BE28754	78.30852	38.92642	Arenite	6	607	26	999	10	Cfa	Blue Ridge
EPP18	BE28755	78.30779	38.93028	Arenite	3	547	14	974	11	Cfa	Blue Ridge
EPP19	BE28756	78.30289	38.94021	Arenite	6	396	28	980	10	Cfa	Blue Ridge
EPP21	BE28758	78.48763	38.74201	Arenite	2	782	14	1052	9	Cfa	Blue Ridge
EPP22	BE28760	78.48698	38.74238	Arenite	3	770	15	1052	9	Cfa	Blue Ridge
EPP23	BE28761	78.55121	38.69810	Arenite	7	793	13	1077	9	Dfa	Blue Ridge
EPP24	BE28762	78.55103	38.69830	Arenite	6	788	16	1077	9	Dfa	Blue Ridge
EPP26	BE28763	78.70035	38.47895	Sandstone	3	861	12	1098	9	Cfa	Blue Ridge
EPP27	BE28764	78.69967	38.48009	Sandstone	5	851	3	1112	9	Cfa	Blue Ridge
EPP31	BE28768	79.24008	38.46995	Sandstone	2	1282	15	1235	7	Dfa	Valley & Ridge
EPP32	BE28769	79.24036	38.46958	Sandstone	4	1290	13	1235	7	Dfa	Valley & Ridge
EPP35	BE28773	78.68158	38.92576	Arenite	2	881	12	1066	8	Dfa	Valley & Ridge
EPP36	BE28774	78.67994	38.92479	Arenite	4	864	13	1011	9	Dfa	Valley & Ridge
EPP37	BE28775	78.71337	38.90656	Sandstone	2	759	18	1011	9	Dfa	Valley & Ridge
EPP38	BE28776	78.71312	38.90709	Sandstone	4	776	7	1011	9	Dfa	Valley & Ridge
EPP39	BE28777	78.90575	38.90126	Sandstone	3	876	23	1077	8	Dfa	Valley & Ridge
EPP40	BE28778	78.90549	38.90170	Sandstone	5	875	17	1077	8	Dfa	Valley & Ridge
EPP41	BE28779	78.89387	38.91569	Sandstone	8	951	1	1116	8	Dfa	Valley & Ridge
EPP42	BE28780	78.89413	38.91539	Sandstone	2	949	9	1116	8	Dfa	Valley & Ridge
EPP43	BE28782	79.36560	38.83581	Sandstone	3	736	68	1011	10	Dfb	Valley & Ridge
EPP44	BE28783	79.36555	38.83591	Sandstone	4	730	57	1011	10	Dfb	Valley & Ridge
EPP45	BE28784	79.25528	38.97292	Sandstone	3	952	35	1155	8	Dfb	Valley & Ridge
EPP46	BE28785	79.25539	38.97279	Sandstone	4	944	44	1155	8	Dfb	Valley & Ridge
EPP47	BE28786	79.25916	38.96392	Sandstone	1	927	35	1134	8	Dfb	Valley & Ridge
EPP48	BE28787	79.25930	38.96333	Sandstone	1	920	80	1134	8	Dfb	Valley & Ridge
EPS03	BE28790	77.65526	40.25835	Sandstone	3	594	14	1047	9	Dfa	Valley & Ridge
EPS04	BE28791	77.65564	40.25779	Sandstone	1	603	10	1082	8	Dfa	Valley & Ridge
EPS05	BE28793	77.67770	40.43601	Conglomerate	1	509	8	1055	8	Dfa	Valley & Ridge
EPS06	BE28794	77.67752	40.43613	Conglomerate	1	507	7	1055	8	Dfa	Valley & Ridge
EPS07	BE28795	77.75675	40.54408	Sandstone	3	583	10	1041	8	Dfa	Valley & Ridge
EPS08	BE28796	77.75827	40.54309	Sandstone	2	585	10	1041	8	Dfa	Valley & Ridge
EPS11	BE28799	78.12403	40.92370	Sandstone	2	571	2	1023	7	Dfb	Appalachian Plateau
EPS12	BE28800	78.12404	40.92369	Sandstone	4	571	2	1023	7	Dfb	Appalachian Plateau
EPS13	BE28801	78.49061	41.14231	Sandstone	2	681	7	1118	6	Dfb	Appalachian Plateau
EPS14	BE28802	78.49048	41.14241	Sandstone	2	674	9	1118	6	Dfb	Appalachian Plateau
EPS15	BE28804	78.49029	41.14255	Sandstone	1	672	4	1118	6	Dfb	Appalachian Plateau
EPS16	BE28805	77.05495	40.37026	Sandstone	2	367	6	1066	10	Dfa	Valley & Ridge
EPS17	BE28806	77.04499	40.37362	Sandstone	7	346	7	1060	10	Dfa	Valley & Ridge
EPS18	BE28807	77.04110	40.37573	Sandstone	3	323	39	1048	10	Dfa	Valley & Ridge
EPS19	BE28808	77.34778	40.04329	Schist	2	488	3	1098	9	Dfa	Blue Ridge
EPS20	BE28809	77.34759	40.04349	Schist	4	488	3	1098	9	Dfa	Blue Ridge
EPS21	BE28810	77.26745	40.03235	Quartzite	4	403	25	1083	10	Dfa	Blue Ridge
EPS22	BE28811	77.26721	40.03252	Quartzite	5	406	20	1083	10	Dfa	Blue Ridge
EPS23	BE28812	77.26730	40.03252	Quartzite	5	407	29	1083	10	Dfa	Blue Ridge
EPS24	BE28813	76.41276	39.63543	Schist	4	160	43	1112	11	Cfa	Piedmont
EPS25	BE28815	76.41260	39.63556	Schist	2	157	43	1112	11	Cfa	Piedmont
EPS26	BE28816	76.41283	39.63546	Quartz Vein	5	162	39	1112	11	Cfa	Piedmont
Spur Ridge Outcrops											
EPP20	BE28757	78.29897	38.94517	Sandstone	2	333		956	11	Cfa	Blue Ridge
EPP28	BE28765	79.56098	38.62863	Sandstone	2	836		1096	9	Dfb	Valley & Ridge
EPP29	BE28766	79.56072	38.62846	Sandstone	2	851		1096	9	Dfb	Valley & Ridge
EPP30	BE28767	79.56027	38.62862	Sandstone	2	867		1096	9	Dfb	Valley & Ridge
EPP33	BE28771	79.19068	38.46645	Sandstone	2	836		1035	9	Dfa	Valley & Ridge
EPP34	BE28772	79.18474	38.46374	Sandstone	3	809		1035	9	Dfa	Valley & Ridge
EPS01	BE28788	77.64166	40.23536	Sandstone	6	574		1099	8	Dfa	Valley & Ridge
EPS02	BE28789	77.64129	40.23520	Sandstone	4	578		1099	8	Dfa	Valley & Ridge
EPS09	BE28797	77.75514	40.76299	Sandstone	7	416		1024	8	Dfa	Valley & Ridge
EPS10	BE28798	77.75477	40.76294	Sandstone	2	419		1024	8	Dfa	Valley & Ridge

*Identification reference number for each sample within the sample database at the Center for Mass Spectrometry at Lawrence Livermore National Laboratory, Livermore, California. Samples were analyzed in April, 2010.

†Elevation and relief data taken from the National Elevation Dataset (ned.usgs.gov). Resolution of 1/3 arcsecond (10m).

§Relief is measured in change in elevation, given in meters, within a 50 m radius of the sampled outcrop.

#Mean Annual Precipitation and Temperature data from Hijmans et al. (2005).

**Climate zone as designated by the Köppen-Geiger climate classification system (Peel et al., 2005). Cfa = Temperate with hot summers without a dry season. Dfa = Cold with hot summers without a dry season. Dfb = Cold with warm summers without a dry season.

TABLE A2. PRINCIPLE COMPONENT ANALYSIS RESULTS

	Eigenvectors				
Parameter	**pc1**	**pc2**	**pc3**	**pc4**	**pc5**
Elevation (masl)	0.65320	0.15759	-0.28357	-0.22208	0.64712
Mean Annual Precipitation (mm yr^{-1})	0.46806	-0.07411	0.55457	0.68362	0.02320
Mean Annual Temperature (°C)	-0.54681	0.42146	-0.03607	0.42963	0.58094
Latitude (°N)	-0.23501	-0.68117	0.41076	-0.26288	0.49289
Relief (m)*	0.00370	0.57275	0.66484	-0.47923	-0.01635
Percent	40	30	16	13	1

*Relief is measured in change in elevation, given in meters, within a 50m radius of the sampled outcrop

TABLE A3. PRINCIPLE COMPONENT VALUES					
Sample	**Principle Component 1**	**Principle Component 2**	**Principle Component 3**	**Principle Component 4**	**Principle Component 5**
		Main Ridgeline Samples			
EPP01	-1.90321	0.25221	-1.00718	0.71215	0.03133
EPP02	-1.89978	0.35888	-0.88586	0.62296	0.03067
EPP04	-0.70708	-0.16314	0.14385	1.05423	-0.04171
EPP05	-0.66067	-0.36207	-0.12269	1.21535	0.01059
EPP06	-0.65798	-0.36129	-0.12392	1.21451	0.01310
EPP07	-0.69933	-0.19625	0.09940	1.08110	-0.03303
EPP08	-0.95193	0.16153	0.35005	0.44301	-0.04290
EPP09	-0.92112	0.02853	0.17258	0.55028	-0.00776
EPP10	-0.74364	-0.18004	0.18373	0.95900	0.00904
EPP11	-1.17917	-0.31241	-0.43003	0.59039	-0.07038
EPP12	-1.71098	0.81481	-0.52130	0.12686	0.26712
EPP13	-1.19929	0.43170	-0.38520	0.00583	-0.19408
EPP14	0.19952	-0.51626	0.42383	0.90198	-0.12093
EPP15	0.25130	-0.57536	0.31999	0.94249	-0.06573
EPP16	0.20648	-0.68996	0.21562	1.04688	-0.10846
EPP17	-0.93861	1.29737	-0.85587	-0.77119	-0.03133
EPP18	-1.74454	1.19144	-1.57000	-0.36453	0.26058
EPP19	-1.66948	1.24810	-0.72767	-0.89572	-0.58346
EPP21	0.47402	0.75676	-1.05611	-0.14148	-0.10634
EPP22	0.44251	0.78402	-1.00129	-0.16034	-0.13842
EPP23	0.74165	0.73321	-0.86734	0.22227	-0.09463
EPP24	0.72909	0.83553	-0.73883	0.13825	-0.11056
EPP26	1.17897	0.91244	-0.88342	0.54445	-0.05230
EPP27	1.27620	0.56804	-1.09011	1.00229	-0.06235
EPP31	4.36247	0.45307	0.26867	1.22438	0.20870
EPP32	4.38321	0.38804	0.17752	1.27629	0.23135
EPP35	1.22112	0.23775	-0.97253	-0.38144	-0.16266
EPP36	0.26302	0.66430	-1.52677	-0.78908	0.21183
EPP37	-0.00674	0.79042	-1.21229	-0.83593	-0.07940
EPP38	0.03539	0.41323	-1.68126	-0.52711	-0.02361
EPP39	1.31720	0.62890	-0.41327	-0.54795	-0.19814
EPP40	1.31306	0.41649	-0.65724	-0.37035	-0.19443
EPP41	1.85619	-0.16725	-0.97490	0.54080	0.04674
EPP42	1.85284	0.11357	-0.64563	0.30689	0.03328
EPP43	-0.45246	2.92504	0.79184	-1.93493	0.20835
EPP44	-0.47081	2.53362	0.34894	-1.60536	0.20382
EPP45	2.19939	0.92305	0.86180	0.03002	0.07057
EPP46	2.18040	1.23513	1.23891	-0.22805	0.04055

EPP47	1.94740	0.94533	0.66151	-0.22040	-0.01003
EPP48	1.93938	2.52670	2.50935	-1.54034	-0.07395
EPS03	-0.54655	-0.74745	-0.05508	-0.57591	0.40777
EPS04	0.21030	-1.25487	0.17155	-0.33500	0.00547
EPS05	-0.33725	-1.51020	0.00806	-0.60983	-0.13158
EPS06	-0.34279	-1.54681	-0.03048	-0.57860	-0.13571
EPS07	-0.30201	-1.47195	-0.08425	-0.95736	0.12512
EPS08	-0.29643	-1.46977	-0.08709	-0.95880	0.12968
EPS11	-0.19874	-2.40709	-0.35182	-1.41098	-0.09912
EPS12	-0.19874	-2.40708	-0.35183	-1.41097	-0.09913
EPS13	1.29680	-2.81990	0.88833	-0.81489	-0.07449
EPS14	1.27878	-2.75399	0.97818	-0.86761	-0.09471
EPS15	1.27233	-2.93153	0.77608	-0.71849	-0.09481
EPS16	-1.42988	-0.98049	0.11432	0.40247	0.35111
EPS17	-1.54004	-0.95315	0.11713	0.31176	0.29484
EPS18	-1.70202	0.17469	1.32522	-0.76933	0.19867
EPS19	-0.30132	-1.07761	0.04108	0.58976	0.02204
EPS20	-0.30138	-1.07779	0.04119	0.58969	0.02217
EPS21	-1.07071	-0.00233	0.84432	0.15330	0.20913
EPS22	-1.06399	-0.17672	0.63652	0.29793	0.22210
EPS23	-1.05931	0.14097	1.00341	0.03175	0.21566
EPS24	-1.73915	1.12319	1.92021	0.69130	-0.24893
EPS25	-1.74710	1.12116	1.92372	0.69394	-0.25668
EPS26	-1.73480	0.98352	1.75437	0.80740	-0.23967

References Cited

Balco, G., Stone, J. O., Lifton, N. A., and Dunai, T. J., 2008, A complete and easily accessible means of calculating surface exposure ages or erosion rates from ^{10}Be and ^{26}Al measurements: Quaternary Geochronology, v. 3, p. 174-195.

Bierman, P., and Nichols, K. K., 2004, Rock to sediment - slope to sea with ^{10}Be - rates of landscape change: Annual Review of Earth and Planetary Sciences, v. 32, p. 215-255.

Bierman, P. R., and Caffee, M., 2001, Slow rates of rock surface erosion and sediment production across the Namib Desert and Escarpment, Southern Africa: American Journal of Science, v. 301, no. April/May, p. 326-358.

-, 2002, Cosmogenic exposure and erosion history of Australian bedrock landforms: GSA Bulletin, v. 114, no. 7, p. 787-803.

Bierman, P. R., Reuter, J. M., Pavich, M., Gellis, A. C., Caffee, M. W., and Larsen, J., 2005, Using cosmogenic nuclides to contrast rates of erosion and sediment yield in a semi-arid, arroyo-dominated landscape, Rio Puerco Basin, New Mexico: Earth Surface Processes and Landforms, v. 30, p. 935-953.

Cerling, T. E., 1990, Dating geomorphologic surfaces using cosmogenic ^{3}He: Quaternary Research, v. 33, p. 148-156.

Cockburn, H. A. P., Brown, R. W., Summerfield, M. A., and Seidl, M. A., 2000, Quantifying passive margin denudation and landscape development using a combined fission-track thermochronology and cosmogenic isotope analysis approach: Earth and Planetary Science Letters, v. 179, p. 429-435.

Craig, H., and Poreda, R. J., 1986, Cosmogenic ^{3}He in terrestrial rocks: the summit lavas of Maui: Proceedings of the National Academy of Sciences, v. 83, p. 1970-1974.

DiBiase, R. A., Whipple, K. X., Heimsath, A. M., and Ouimet, W. B., 2010, Landscape form and millennial erosion rates in the San Gabriel Mountains, CA: Earth and Planetary Science Letters, v. 289, p. 134-144.

Elmore, D., and Phillips, F. M., 1987, Accelerator Mass Spectrometry for Measurement of Long-Lived Radioisotopes: Science, v. 236, no. 4801, p. 543-550.

Hijmans, R. J., Cameraon, S. E., Parra, J. L., Jones, P. G., and Jarvis, A., 2005, Very high resolution interpolated climate surfaces for global land areas: International Journal of Climatology, v. 25, 0. 1965-1978.

Gosse, J. C., and Phillips, F. M., 2001, Terrestrial in situ cosmogenic nuclides: theory and application: Quaternary Science Reviews, v. 20, p. 1475-1560.

Kohl, C. P., and Nishiizumi, K., 1992, Chemical isolation of quartz for measurement of *in-situ*-produced cosmogenic nuclides: Geochimica et Cosmochimica Acta, v. 56, p. 3583-3587.

Kurz, M. D., 1986, Cosmogenic helium in a terrestrial igneous rock: Nature, v. 320, no. 3, p. 435-439.

Lal, D., 1991, Cosmic ray labeling of erosion surfaces: *in situ* nuclide production rates and erosion models: Earth and Planetary Science Letters, v. 104, p. 424-439.

Nishiizumi, K., Imamura, M., Caffee, M. W., Southon, J. R., Finkel, R. C., and McAninch, J., 2007, Absolute calibration of ^{10}Be AMS standards: Nuclear Instruments and Methods in Physics Research B, v. 258, p. 403-413.

Nishiizumi, K., Kohl, C. P., Arnold, J. R., Klein, J., Fink, D., and Middleton, R., 1991, Cosmic ray produced ^{10}Be and ^{26}Al in Antarctic rocks: exposure and erosion history: Earth and Planetary Science Letters, v. 104, p. 440-454.

Portenga, E. W., and Bierman, P. R., 2011, Understanding Earth's eroding surface with ^{10}Be: GSA Today, v. 21, no. 8, p. 4-10.

Safran, E. B., Bierman, P. R., Aalto, R., Dunne, T., Whipple, K. X., and Caffee, M., 2005, Erosion rates driven by channel network incision in the Bolivian Andes: Earth Surface Processes and Landforms, v. 30, p. 1007-1024.

Schaller, M., Blanckenburg, F. v., Hovius, N., and Kubik, P. W., 2001, Large-scale erosion rates from in situ-produced cosmogenic nuclides in European river sediments: Earth and Planetary Science Letters, v. 188, p. 441-458.

Stone, J. O., 2000, Air pressure and cosmogenic isotope production: Journal of Geophysical Research, v. 105, no. B10, p. 23,753-23,759.